

Waldenström macroglobulinemia whole genome reveals prolonged germinal center activity and late copy number aberrations

Kylee H. Maclachlan,^{1,*} Tina Bagratuni,^{2,*} Efstathios Kastritis,² Bachisio Ziccheddu,³ Sydney Lu,⁴ Venkata Yellapantula,⁵ Chris Famulare,⁶ Kimon Argyropoulos,⁷ Andriy Derkach,⁸ Elli Papaemmanuil,⁸ Ahmet Dogan,⁹ Alexander Lesokhin,^{1,10} Saad Z. Usmani,¹ C. Ola Landgren,^{3,†} Lia M. Palomba,^{7,10,†} Francesco Maura,^{3,†} and Meletios A. Dimopoulos^{2,†}

¹Myeloma Service, Department of Medicine, Memorial Sloan Kettering Cancer Center, New York, NY; ²Department of Clinical Therapeutics, National and Kapodistrian University of Athens School of Medicine, Athens, Greece; ³Myeloma Division, Sylvester Comprehensive Cancer Center, University of Miami, Miami, FL; ⁴Department of Medicine, Stanford University, Stanford, CA; ⁵Department of Bioinformatics, Children's Hospital of Los Angeles, Los Angeles, CA; ⁶Center for Hematologic Malignancies, Memorial Sloan Kettering Cancer Center, New York, NY; ⁷Lymphoma Service, Department of Medicine, Memorial Sloan Kettering Cancer Center, New York, NY; ⁸Department of Epidemiology and Biostatistics, Memorial Sloan Kettering Cancer Center, New York, NY; ⁹Hematopathology Service, Department of Pathology, Memorial Sloan Kettering Cancer Center, New York, NY; ¹⁰Department of Medicine, Weill Cornell Medical College, New York, NY

Key Points

- WGS reveals that precursors with low genomic complexity have a lower risk for progression to WM.
- Molecular time analysis shows chr12 gain occurred early in development, whereas other gains occur later and may be associated with progression.

The genomic landscape of Waldenström macroglobulinemia (WM) is characterized by somatic mutations in *MYD88*, present from the precursor stages. Using the comprehensive resolution of whole genome sequencing (WGS) in 14 CD19-selected primary WM samples; comparing clonal and subclonal mutations revealed that germinal center (GC) mutational signatures SBS9 (poly-eta) and SBS84 (AID) have sustained activity, suggesting that the interaction between WM and the GC continues over time. Expanding our cohort size with 33 targeted sequencing samples, we interrogated the WM copy number aberration (CNA) landscape and chronology. Of interest, CNA prevalence progressively increased in symptomatic WM and relapsed disease when compared with stable precursor stages, with stable precursors lacking genomic complexity. Two *MYD88* wild-type WGS contained a clonal gain affecting chromosome 12, which is typically an early event in chronic lymphocytic leukemia. Molecular time analysis demonstrated that both chromosomal 12 gain events occurred early in cancer development whereas other CNA changes tend to occur later in the disease course and are often subclonal. In summary, WGS analysis in WM allows the demonstration of sustained GC activity over time and allows the reconstruction of the temporal evolution of specific genomic features. In addition, our data suggest that, although *MYD88*-mutations are central to WM clone establishment and can be observed in precursor disease, CNA may contribute to later phases, and may be used as a biomarker for progression risk from precursor conditions to symptomatic disease.

Introduction

Waldenström macroglobulinemia (WM) is an immunoglobulin M (IgM)-producing indolent B-cell lymphoma, existing on a clinical spectrum from precursor states (IgM monoclonal gammopathy of uncertain

Submitted 6 September 2022; accepted 25 October 2022; prepublished online on *Blood Advances* First Edition 4 November 2022; final version published online 17 March 2023. <https://doi.org/10.1182/bloodadvances.2022008876>.

*K.H.M. and T.B. contributed equally to this work.

†C.O.L., M.L.P., F.M., and M.A.D. contributed equally to this work.

WGS data will be made available upon publication, please contact: Kylee H. Maclachlan (maclachk@mskcc.org). Targeted sequencing data are available via the cBioportal for Cancer Genomics (<http://cbiportal.org/msk-impact>).

Presented in abstract form at the 63rd annual meeting of the American Society of Hematology, Atlanta, GA, 11-14 December 2021.

The full-text version of this article contains a data supplement.

© 2023 by The American Society of Hematology. Licensed under [Creative Commons Attribution-NonCommercial-NoDerivatives 4.0 International \(CC BY-NC-ND 4.0\)](https://creativecommons.org/licenses/by-nc-nd/4.0/), permitting only noncommercial, nonderivative use with attribution. All other rights reserved.

significance [MGUS] and asymptomatic WM) to symptomatic disease.¹ The genomic landscape of WM is characterized by recurrent somatic mutations in *MYD88*, producing increased signaling through Bruton's tyrosine kinase (BTK) and nuclear factor kappa B activation, which promote WM growth and survival.¹⁻³ *MYD88*^{L265P} mutations are not specific to WM, occurring in a majority of primary central nervous system and testicular lymphomas and a minority of marginal zone and nongermlinal-center (GC) diffuse large B-cell lymphomas.^{4,5} Though highly prevalent in WM, *MYD88*^{L265P} mutations are not sufficient for progression to symptomatic disease, occurring in IgM MGUS and both stable asymptomatic and symptomatic WM.^{4,6} This distribution suggests that *MYD88* mutation is an early event in clonal development, potentially acquired before the first GC encounter,⁷ whereas other genomic events promote subsequent cancer progression.

WM wild-type (wt) for *MYD88*^{L265P} has an estimated prevalence below 10%.⁸ The lack of *MYD88*^{L265P} produces diagnostic uncertainty, and this entity is not well characterized genomically, with some tumor features overlapping with other low-grade lymphomas, including marginal zone lymphoma and chronic lymphocytic leukemia (CLL).

Other recurrent somatic mutations described, predominantly detected by targeted sequencing, include *CXCR4*, *ARID1A*, *CD79B*, *NOTCH2*, *MLL2*, *KMT2D*, and *TP53*, many of which also occur in WM precursor states.² Indeed, Paiva et al have demonstrated that there are almost no genes showing significantly different dysregulation when comparing IgM MGUS and asymptomatic WM to symptomatic WM.⁹ Clinically, although most mutations have an unclear impact on prognosis, once treatment is indicated, responses to BTK-signaling inhibitors are affected by *MYD88* and *CXCR4* mutational status.^{10,11}

Specific copy number aberrations (CNA) are highly recurrent in WM, with del6q resulting in loss of genes that modulate BTK and NFκB signaling (*IBTK*, *TNFAIP3*, *HIVEP3*) as well as cell survival/apoptotic balance (*BCLAF1*, *FOXO3*).^{2,12} Del6q in WM precursors has been associated with a shorter time to requiring treatment and shorter progression-free survival once treatment is initiated.¹³

The increased resolution gained from WGS in comparison to targeted sequencing allows a comprehensive characterization of mutational processes (ie, mutational signatures) and structural variation (SV) contributing to cancer pathogenesis, in addition to detailing single base substitution (SBS) and CNA.^{14,15} In the context of multiple myeloma (MM), targeted and whole exome sequencing defined some genomic features predicting progression from precursor states to symptomatic MM, including *KRAS/NRAS* mutations, *TP53* deficiency, and *MYC* aberrancy.^{16,17} WGS analysis has allowed us to extend these findings and demonstrate that precursor states that subsequently progress to MM already have MM-defining genomic events, including the complex SV chromothripsis, specific CNA, templated insertions, and APOBEC-mutational activity (SBS signatures SBS2/SBS13).¹⁸ WGS data, therefore, allow the distinction of 2 biologically and clinically distinct entities; either stable or progressive precursors.

WGS allows the differentiation between clonal and subclonal events, and in addition, in tumors with large chromosomal gains,

can provide insight into the temporal acquisition of genomic clonal events. We have demonstrated in MM how utilizing the corrected ratio between clonal mutations being either duplicated (present on both alleles and therefore acquired before the gain) or nonduplicated (present on a single allele, acquired postgain) within large chromosomal gains provides a molecular time estimation.¹⁹⁻²¹ Using this approach, we've shown that hyperdiploid copy number profiles in MM may be acquired in multiple time windows.^{19,21}

In this article, we aim to characterize the temporal relationship between SBS mutational signatures, CNA, and SV in WM, using the comprehensive resolution afforded by WGS. We examined WGS from 14 CD19-selected primary samples from patients with WM, together with 33 samples from WM having targeted sequencing available.²² Our data show that GC mutational signatures are present in both clonal and subclonal populations, demonstrating that GC activity is sustained over a period of time. Both SBS landscape and mutational drivers predict clinical stage poorly. In contrast, SV and CNA emerged as key drivers to later phases and disease progression. Finally, WGS from *MYD88*-wt cases suggests that B-cell post-GC precursor clones may develop early gains in chromosome 12, with a later trajectory leading to either CLL or *MYD88*-wt WM.

Methods

Patient samples

This study involved the use of human samples, which were collected after written informed consent was obtained. Institutional review boards at each site approved the study, with samples and data obtained and managed in accordance with the Declaration of Helsinki. Patient details are summarized in supplemental Table 1.

DNA was extracted from CD19⁺ cells purified from the bone marrows of 14 patients collected at the University of Athens, with matched normal samples collected from peripheral blood mononuclear cells. Samples were collected at different clinical time points: MGUS (n = 1), asymptomatic WM (n = 5), symptomatic (n = 7), and relapsed WM (n = 1), with sequencing depth detailed in supplemental Table 2.

Previously published targeted sequencing data were obtained from 33 patients with WM at Memorial Sloan Kettering Cancer Center,^{22,23} predominantly from bone marrow (n = 13) and lymph node biopsies (n = 10), with the remainder from extramedullary disease (n = 6), peripheral blood (n = 3), and cerebrospinal fluid (n = 1). Again, there was a range of clinical scenarios, comprising stable asymptomatic (n = 5), asymptomatic which progressed during follow-up (n = 2), symptomatic but untreated (n = 9), and treatment-exposed WM (n = 17) (supplemental Table 1).

Genomic sequencing

For each WGS sample, 500ng of genomic DNA was sheared and sequencing libraries were prepared using the KAPA Hyper Prep Kit (KAPA Biosystems). Samples were run on a NovaSeq 6000 in a 150bp/150bp paired-end runs, using the SBS v1 Kit and an S4 flow cell (Illumina). The average sequence coverage was 69 for tumor samples and 35 for normal samples (supplemental Table 2). All new sequencing data will be available on publication.

The targeted sequencing data were produced using the MSK-IMPACT Heme gene panel,²² with all data previously published^{23,24} and accessible in the cBioportal for Cancer Genomics (<http://cbioportal.org/msk-impact>).²⁵ Copy number aberration had been previously defined by Fraction and Allelic Copy number Estimation from Tumor/normal Sequencing.²⁶

Bioinformatic analysis

All WGS bioinformatics analyses were performed using our in-house pipeline Isabl.²⁷ Short-insert paired-end reads were aligned to the reference human genome (GRCh37) using Burrows-Wheeler Aligner (v0.7.8). Somatic mutations were identified by CaVEman.²⁸ To detect genes and hotspots under positive selection in our cohort we applied the *dndscv* method. This algorithm was designed to detect genes under positive selection, even in small datasets (<https://github.com/im3sanger/dndscv>).²⁹ The background mutation rate across each gene is estimated from synonymous mutations within the gene using the variation of mutation rates across genes. The detection of positive selection is further enhanced by controlling the input in restricted hypothesis testing to a set of known relevant oncogenes rather than all available genes (ie, the MSK-IMPACT Heme gene panel²²).

Copy number analysis and tumor purity (ie, cancer cell fraction) were evaluated using Battenberg (<https://github.com/Wedge-Oxford/battenberg>), with significantly aberrant regions identified using GISTIC2.0 (v2.0.23, <https://www.genepattern.org>). SVs were defined by merging calls from SvABA,³⁰ BRASS (<https://github.com/cancerit/BRASS>), and GRIDSS analyses (<https://github.com/PapenfussLab/gridss>). Complex events were defined and annotated as previously described.²¹ The phylogenetic tree of each case was reconstructed using the Dirichlet process (<https://github.com/Wedge-Oxford/dpclus>).

To estimate the activity of mutational signatures, we followed our recently published workflow based on 3 steps: de novo extraction, assignment, and fitting.^{31,32} For the first step, we ran *SigProfiler*.³¹ Then all extracted signatures were compared with the latest COSMIC reference (<https://cancer.sanger.ac.uk/cosmic/signatures/SBS/>) in order to define which known mutational processes were active in our cohort. Finally, we applied *mmsig* (<https://github.com/UM-Myeloma-Genomics/mmsig>), a fitting algorithm designed for MM, to confirm the presence and estimate the contribution of each mutational signature in each sample.³³ Confidence intervals were generated by drawing 1000 mutational profiles from the multinomial distribution, each time repeating the signature fitting procedure, and finally taking the 2.5th and 97.5th percentile for each signature. To explore the contribution of each mutational signature over time, we explore all Dirichlet process clusters with more than 30 mutations using *mmsig* as described above.

The relative timing of each multichromosomal gain event was estimated using the R package *mol_time* (https://github.com/UM-Myeloma-Genomics/mol_time).^{19,21} Correcting the ratio between duplicated mutations (variant allele frequency around 66%, acquired before the chromosomal duplication) and nonduplicated mutations (variant allele frequency around 33%, acquired on either the nonduplicated allele or on one of the 2 duplicated ones). This approach allows for estimation of the relative molecular time of acquisition of all large (>1 Mb) chromosomal gains with adequate clonal mutations as estimated by the Dirichlet process.

Data analysis and statistics

Analysis was carried out in R version 3.6.1. Key software tools noted throughout the workflow (including *SigProfiler*, *mmsig*, *dndscv* and *mol_time*) are publicly available.

Results

Experimental data and design

We performed WGS on 14 primary bone marrow samples from patients with WM at various clinical stages, including IgM monoclonal gammopathy (MGUS, $n = 1$), asymptomatic ($n = 5$), symptomatic ($n = 7$), and relapsed WM ($n = 1$). These data were compared with targeted sequencing on 33 patients with WM, of whom 5 were stable precursors, using the MSK-IMPACT Heme gene panel (400-570 genes depending on assay version).²² Patient characteristics are shown in supplemental Table 1, with progression-free survival of asymptomatic patients detailed in supplemental Figure 1 (median, 2.2 years; interquartile range [IQR], 2.1-2.3 years).

Mutational landscape in WM reveals sustained GC interaction

WGS from 14 patients with WM identified a median of 2806 clonal SBS per sample (IQR, 1870-3079). 12 out of 14 (85%) samples harbored *MYD88* mutations.

To identify recurrent nonsynonymous mutations occurring at a higher than expected rate by chance alone, we ran *dndscv*,²⁹ performing analysis against both an unrestricted background and a restricted hypothesis for 570 known oncogenic drivers, selected because of their inclusion in the MSK-IMPACT Heme panel. Twenty mutations in 5 driver genes were extracted, which in addition to *MYD88* included *CXCR4* (3/14), *CD79B* (2/14), *HIST1H1D* (2/14) and *HIST1H1D* (2/14) (supplemental Table 3). Examination of known oncogenic hotspots using *dndscv* revealed 4 significant hotspots in the 14 WGS; *MYD88* (L265P), *TP53* (W91*), *PIM1* (K24N), and *EZH2* (Y646F).

Using the ability of WGS to incorporate noncoding DNA and to investigate which mutational processes are involved in shaping the genomic landscape of WM we performed a mutational signature analysis.³¹⁻³³ Four previously reported SBS signatures were detected (Figure 1): SBS1 and SBS5 (associated with aging), SBS9 (reflecting poly-eta activity in the GC), and SBS8 (not yet associated with a known biological process). In line with previous evidence in other malignancies,²¹ the contribution of age-related signatures SBS1/SBS5 was directly correlated with the age at presentation ($R^2 = 0.44$, $P = .014$). When comparing SBS signatures in WM with those observed in MM (Figure 1,^{19,32,34}), we note a striking absence of APOBEC-mutational activity (SBS2/SBS13) in all samples.³⁵ The SBS signature contribution was similar when examining total clonal and subclonal mutations (Figure 2A-C). The signature SBS9 demonstrated sustained GC activity, as evidenced by the same proportion of mutations attributable to SBS9 after collapsing all mutations at each of the clonal and subclonal level (24%, Figure 2C). Examining the 96-class SBS profile and signatures extracted from SBS specific to the immunoglobulin loci, we observed evidence of clustered SBS84 (a signature associated with activation-induced cytidine deaminase

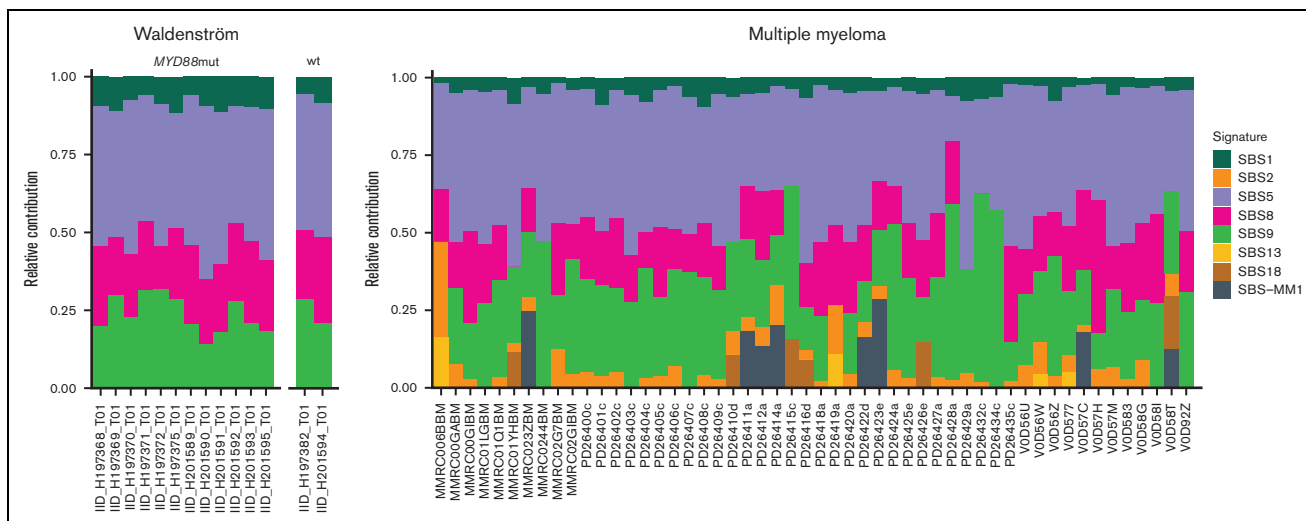


Figure 1. SBS signatures in WM compared with MM.

activity). This reflects somatic hypermutation within the GC with SBS84 accounting for 48% of signature contribution from sub-clonal mutations within immunoglobulin genes (Figure 2D-F). Overall, these data suggest that the interaction between WM and the GC is sustained over time, similar to the early phase of MM¹⁹ and other hematologic malignancies.³⁶

SV and CNA in WM predict progression to symptomatic disease

WGS allows for an accurate definition of SV and complex events, which we have previously demonstrated to be critical for the pathogenesis and clinical outcomes of MM and aggressive lymphomas.³⁷⁻³⁹ Using *IgCaller*⁴⁰ to reconstruct the VDJ and class-switch recombination of each patient immunoglobulin gene, we confirmed that all WGS samples had a productive immunoglobulin H rearrangement and either a productive immunoglobulin K or immunoglobulin L rearrangement consistent with known WM biology⁴¹ (supplemental Table 4). Although, as expected, we documented an absence of oncogenic translocations involving *BCL2*, *CCND1* or *MYC*, 2 potentially oncogenic translocations were included in the *IgCaller* output, t(2;22), IGL - no partner gene identified, and t(4;22), LYAR-IGL, neither of which have clear biological or prognostic impact in WM. These 2 translocations both occurred in *MYD88*-mut cases with symptomatic WM.

In contrast to MM,³⁷ in this WM WGS cohort we found a low prevalence of complex SV with no chromothripsis detected and a single chromoplexy event found in 3 patients (21%, Figure 3A and supplemental Figure 2), all of whom had symptomatic WM. Chromoplexy is characterized by a concatenation of multiple SV on different chromosomes leading to multiple deletions.^{14,15} These kinds of events are particularly relevant because they allow the tumor cell to acquire multiple genomic drivers at the same time.²¹ Specifically, in sample H201589 (Figure 3A), copy number loss related to a chromoplexy event affected genes including *CDKN2C*, *PRDM1*, *HLA-G*, *ARID2*, and *ARID1B*. In sample H197369 (Figure 3B-C, supplemental Figure 2) chromoplexy affected driver genes *NFKB2* and *MEF2B*, whereas in sample H201593, chromoplexy is linked to del6q. We also note a reciprocal translocation

affecting *NFKB2* in a further patient (H201594, Figure 3D). Overall, there was a low incidence of any SV and fewer SV in asymptomatic precursor samples compared with those having symptomatic disease (Figure 3E).

Targeted sequencing is not able to accurately define SV but allows for the definition of CNA. To explore WM CNA features in a larger cohort, we examined the WGS data together with 33 patients with WM in whom targeted sequencing was available (MSK-IMPACT Heme gene panel [400-570 genes depending on assay version],²² data via cBioportal,²⁵ clinical information in supplemental Table 1). Running GISTIC2.0 we identified focal genomic regions recurrently involved by gains (n = 2) and deletions (n = 3, supplemental Table 5). CNA analysis demonstrated that some samples harbored typical CNA features such as del6q, whereas other tumors had minimal CNA. Cumulative CN profiles comparing samples from stable WM precursors to those with symptomatic or relapsed disease demonstrated significantly increased CN with disease progression, with 6q being significant from GISTIC2.0 analysis, being only detected in symptomatic and relapsed WM and absent among stable WM precursors (Figure 4A-B).¹³

We examined the SBS landscape of known oncogenic drivers, drivers extracted in this WGS cohort by *dndscv*, and mutations previously described in WM literature, and found that they poorly predict clinical stage (Figure 4C). Investigating the genomic landscape of the 2 most recurrent genomic drivers after *MYD88* mutation (ie, *CXCR4* mutation and del6q), no significant differences were observed after correcting for the clinical stage (supplemental Figure 3).

In contrast to the mutational spectra, the combination of CNA with SV provided clear clustering by clinical stage (Figure 4D), with patients having precursor disease that subsequently progressed to symptomatic WM having CNA similar to those having already developed symptomatic disease. These data suggest that, although *MYD88*-mutations are central to WM clone establishment and can be observed in stable precursor disease, CNA and SV may contribute to later phases and disease progression, with certain CNA at the asymptomatic phase predicting subsequent progression.¹³

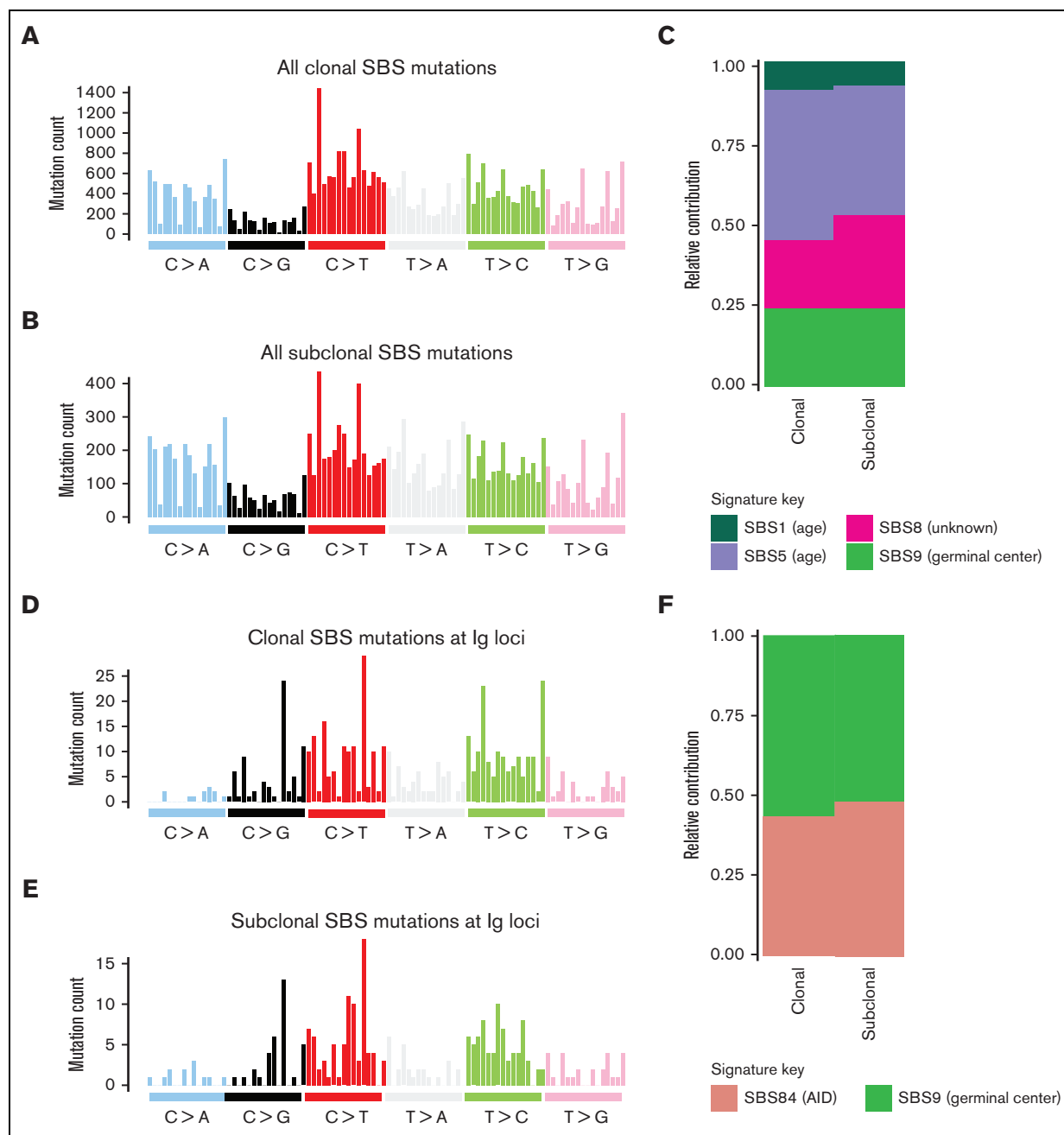


Figure 2. Clonal and subclonal contribution of SBS signatures in WM. 96-class profile of genome-wide SBS mutations at the (A) clonal and (B) subclonal level. (C) SBS mutational signatures obtained after collapsing all genome-wide mutations at the clonal and subclonal level. (D-E) 96-class profile of SBS mutations specific to the immunoglobulin loci at the (D) clonal and (E) subclonal level. (F) SBS mutational signatures obtained after collapsing all mutations within immunoglobulin loci at the clonal and subclonal level.

Molecular time in WM

The proportion of WM wt for *MYD88* has been estimated to be less than 10%.^{8,12} 2 out of 14 of the WGS and 2 out of 33 of the targeted sequencing samples were *MYD88*-wt (8.5% in total), collected from patients producing large amounts of IgM paraprotein (each >2800 mg/dL) and having other mutations previously described in WM, including *ARID1A*, *PIM1*, *TRAF3*, *NOTCH2*, and *KMT2D* (supplemental Table 1). We hypothesized that the resolution of WGS may define additional genomic features relevant

to disease pathogenesis, in particular for patients with *MYD88*-wt. Of interest, the 2 *MYD88*-wt WGS samples both contained a clonal gain affecting chromosome 12 (Figure 5A-B), which is typically an early event in lymphoproliferative disorders such as CLL.²⁰ Other clonal gains affected chromosomes 3, 5, 15, and 16 in the sample of a patient with *MYD88*-wt, with a gain of 3 q and gains of chromosomes 4 and 18 in 2 *MYD88*-mutant samples (Figure 5A-D). To estimate the chronological order of these large chromosomal duplications, we ran a molecular time analysis, which

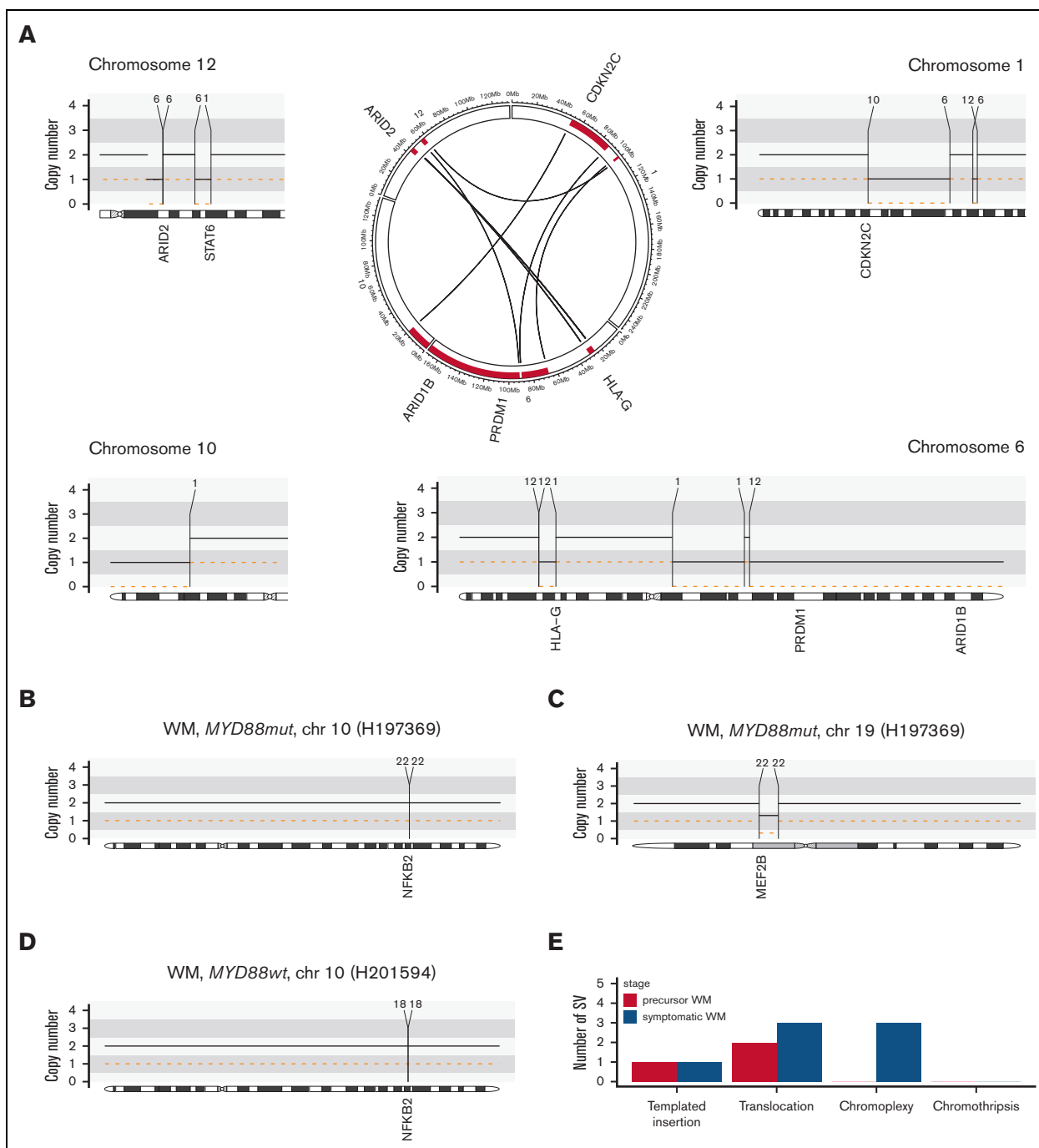


Figure 3. Structural variants in WM. (A) Example of a chromoplexy event between chromosomes 1, 6, 10, and 12. (B-D) Examples of structural variants affecting driver genes: translocations affecting *NFKB2* (B/C) and *MEF2B* (D). (E) Total number of structural variants by disease stage.

uses the corrected ratio between duplicated and nonduplicated clonal mutations within large chromosomal gains in WGS data.¹⁹ This demonstrated that these 2 chromosomal gain events affecting chromosome 12 occurred early in cancer development (molecular time <0.5, Figure 5E-F), similar to the timing of chromosome 12 gains observed in the PCAWG CLL data set²⁰ (median molecular time 0.36, IQR 0.17-0.44, supplemental Figure 4). Multiple other CNA changes occurred later in the disease course (molecular time >0.5) and tended to be subclonal

(Figure 5E-H). We observed that the GC center signature SBS9 is present both in early and late molecular time windows, and in both pregain and postgain populations, suggesting that these large chromosomal gains were acquired within the GC.

Considering the targeted sequencing data, chromosome 12 gains were observed in 3 *MYD88-mt* samples; 2 from patients with symptomatic WM and 1 in a patient who subsequently progressed to symptomatic disease. Targeted sequencing does not allow for

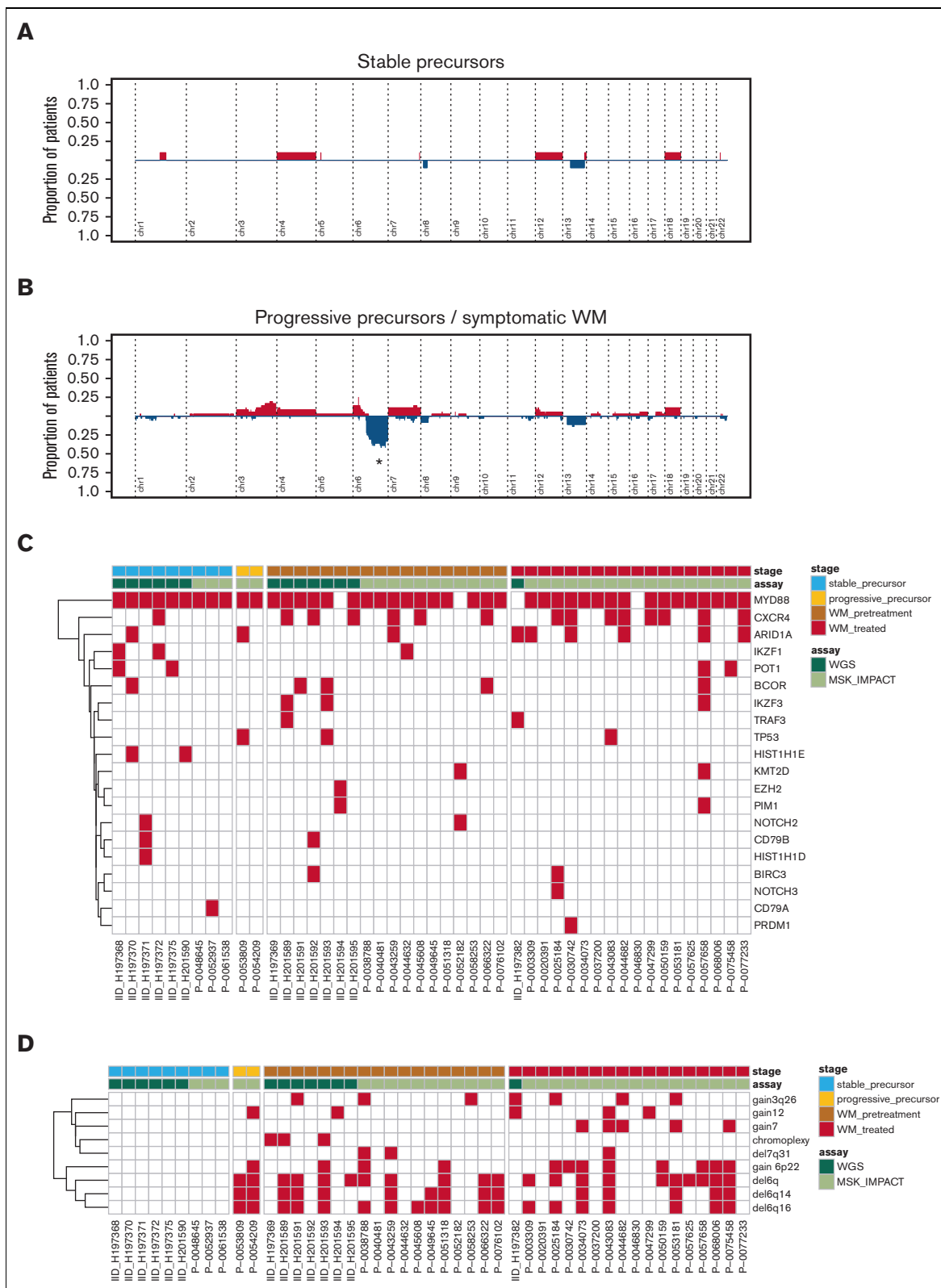


Figure 4. Copy number profiles from Waldenström's macroglobulinemia. Cumulative copy number profiles across samples with (A) IgM MGUS or symptomatic precursor WM, and (B) symptomatic and treatment-exposed Waldenström's macroglobulinemia. Samples from patients with asymptomatic disease that later progressed were considered together with samples from symptomatic patients. In (A/B), red, gain; blue, deletion. * = peak is significantly different between group according to *GISTIC* analysis. (C) Heatmap of mutations according to clinical stage. (D) Heatmap of copy number and structural variants according to clinical stage.

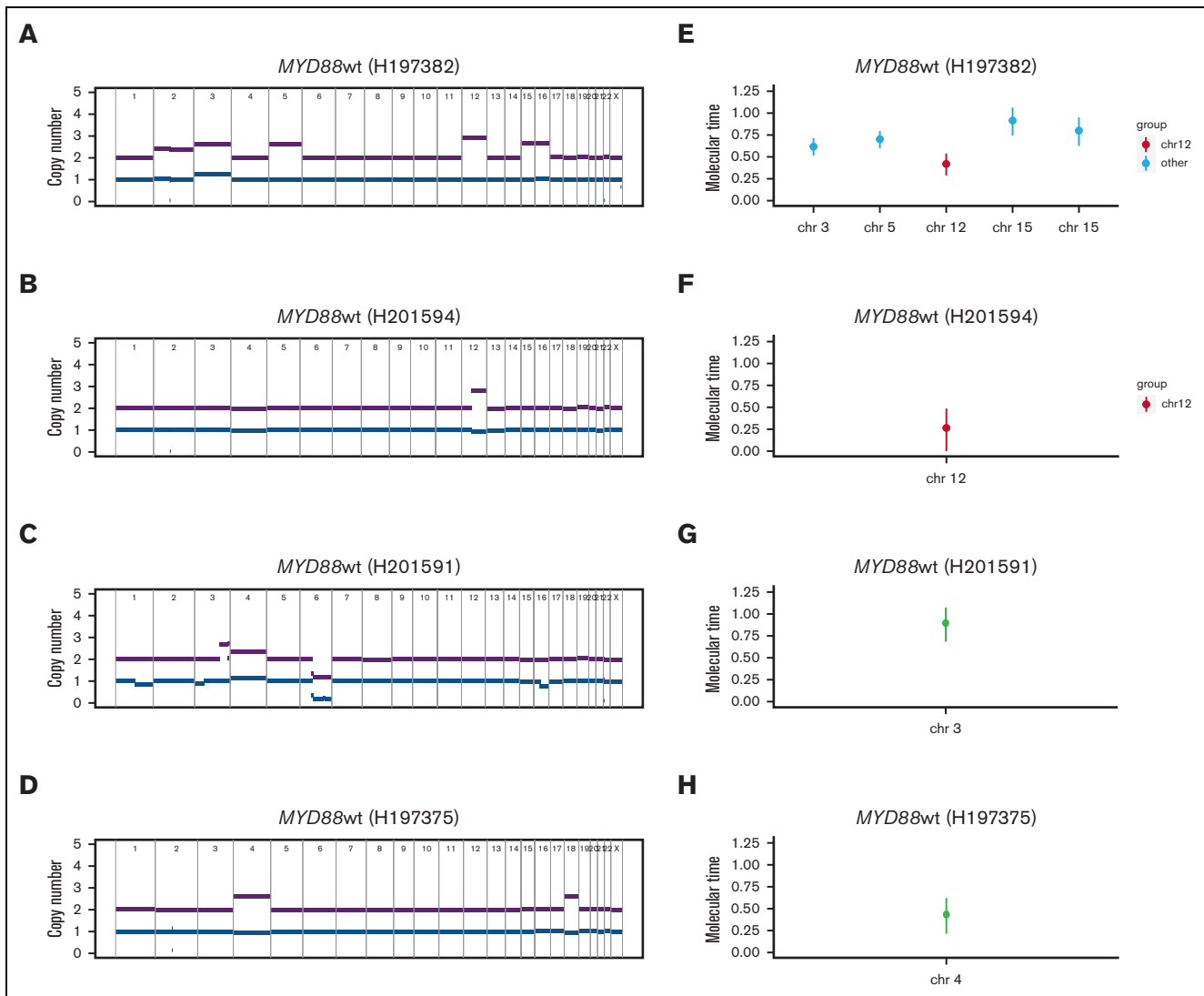


Figure 5. Molecular timing analysis. Copy number profiles from; (A) *MYD88*-wt sample, demonstrating gains in chromosomes 3, 5, 12, 15, 16, (B) *MYD88*-wt sample with gain in chromosome 12, (C) *MYD88*-mutant sample with gain of 3q and (D) *MYD88*-mutant sample with gains of chromosomes 4 and 18. (E-H) Molecular timing analysis for the same 4 patient samples, using the ratio of duplicated:nonduplicated mutations within clonal chromosomal gains. Red, molecular time in chromosome 12 gains; aqua, gains in other chromosomes in patients harboring a chromosome 12 gain; black, other gains.

molecular time analysis, but these data support the hypothesis that CNA predicts later progression. Despite small numbers, taken altogether, our data suggest that precursor B-cell clones may develop gains in chromosome 12 early in cancer development within the GC, with a later trajectory leading to either CLL, *MYD88*-mt WM or *MYD88*-wt disease. Furthermore, they suggest that both deletions and large chromosomal gains tend to play a late driver role and might be used as biomarkers to predict for clinical progression in WM precursor conditions.

Discussion

The discovery of *MYD88* L265P mutations, highly prevalent throughout the disease spectrum of IgM monoclonal gammopathies, revealed this mutation to be an early event in clonal development.² Here, we have used the comprehensive resolution

of WGS to examine for mutational signatures, CNA and structural variants which may contribute to disease development and progression to symptomatic WM.

Traditionally, WM was regarded as a post-GC malignancy, having undergone somatic hypermutation but not class-switch recombination. Recently, Dhodapkar et al published that the establishment of the malignant clone in WM is preceded by an expansion of nonmalignant extrafollicular B cells, with aberrant oncogenic signaling involving *MYD88* in pre-B progenitor cells,⁷ in line with previous early evidence by Paiva et al.⁹ Here, examining the 96-class SBS profile and mutational signatures obtained from clonal and subclonal SBS mutations, we demonstrate that the malignant WM clone continues to interact with the GC over time, with the same proportion of mutations attributable to SBS9 being observed in both the clonal and subclonal fractions.

In order to explore the biological relevance of CNA, we demonstrate the increasing prevalence of CNA in symptomatic WM and relapsed disease when compared with stable precursor stages. Of note, biopsies collected in asymptomatic patients who later progressed to symptomatic disease contained CNA similar to biopsies collected in symptomatic disease. In addition, complex SV was only observed in patients with symptomatic disease. Although some genomic features may be selected for under therapeutic pressure, CNA and SV clustered untreated symptomatic disease together with posttreatment biopsies and distinct from stable precursor states. Similarly to MM,^{18,19} these data suggest that WM precursors demonstrating low genomic complexity, lacking CNA and complex SV, are biologically lower risk for progression to symptomatic disease. This pathophysiology is best appreciated with the increased resolution of WGS data.

Samples from 2 *MYD88*-wt WGS contained a clonal gain affecting chromosome 12, which is typically an early event in CLL, as demonstrated in the PCAWG WGS data set.²⁰ Molecular time analysis demonstrated that these 2 chromosomal gain events occurred early in cancer development whereas other CNA changes occurred later in the disease course. Though observed in only 2 samples, these data demonstrate the additional power of WGS in elucidating biology and suggest that precursor clones may develop gains in chromosome 12 early in cancer development, with multiple potential trajectories, not restricted to CLL.

Considering potential limitations of this study, the relationship between disease history and the timing of sample collection is difficult to evaluate. It is possible that biopsies from stable WM precursors were collected earlier in the disease life history than the progressive ones. Were this to be the case, it would mean that those clones haven't yet acquired large aneuploidies and SV required for tumor progression, and our observations remain valid. We have also included relapsed WM in our study, and as noted above, whereas certain genomic features may be selected as a consequence of exposure to anticancer therapy, CNA and SV clustered symptomatic disease distinct from stable precursor states before the effect of treatment becomes relevant. Although the limited sample size doesn't allow for definitive conclusions, the data presented and exploratory analysis provide both additional support to previous reports^{1,2,8,13,16} and proof-of-principle that the use of WGS and specific computational methods allow for a comprehensive characterization of the WM genomic landscape.

In conclusion, we have 3 main findings from applying advanced analytical techniques to WGS data in WM. First, WGS analysis

allows the demonstration of sustained GC activity in WM over time, supporting an ongoing interaction of the GC with the WM clone. Second, whereas *MYD88*-mutations are central to WM clone establishment and precursor clones may develop gains in chromosome 12 early in cancer development within the GC, additional late CNA may contribute to symptomatic disease progression. Finally, despite the limited number of available samples, our data suggest that in WM, similarly to MM,¹⁸ leveraging the comprehensive genomic characterization provided by WGS, it is possible to differentiate stable WM precursors from those destined to progress over time. Following validation of these findings in a larger cohort, future prognostication in WM precursor disease may be improved by the integration of CN and SV data.

Acknowledgments

This work was supported by the MSK Steven Greenberg Lymphoma Research Awards, Sylvester Comprehensive Cancer Center NCI Core Grant (P30 CA 240139), and the Memorial Sloan Kettering Cancer Center NCI Core Grant (P30 CA 008748). F.M. and K.M. are supported by the American Society of Hematology. F.M. and O.L. are supported by the Riney Family Foundation.

Authorship

Contribution: F.M. and T.D. designed and supervised the study, collected and analyzed the data, and wrote the paper; O.L. and L.P. designed and supervised the study, collected the data, and wrote the paper; K.M. and T.B. collected and analyzed the data and wrote the paper; E.K. collected the data and wrote the paper; S.L., C.F., K.A., A.D., A.L., and S.U., collected the data; and B.Z., V.Y., A.D., and E.P. analyzed the data.

Conflict-of-interest disclosure: The authors declare no competing financial interests.

ORCID profiles: K.H.M., 0000-0001-7873-4854; T.B., 0000-0001-8695-0493; E.K., 0000-0001-8191-5832; K.A., 0000-0003-1510-5887; A. Derkach, 0000-0003-2178-8493; A. Dogan, 0000-0001-6576-5256; A.L., 0000-0001-9321-702X; C.O.L., 0000-0001-6485-4839; F.M., 0000-0002-5017-1620.

Correspondence: Francesco Maura, Myeloma Division, Sylvester Comprehensive Cancer Center, University of Miami, Miami, FL 33136; email: fxm557@med.miami.edu; and Meletios-Athanasios Dimopoulos, National and Kapodistrian University of Athens, Athens, Greece; email: mdimop@med.uoa.gr.

References

1. Treon SP, Xu L, Yang G, et al. *MYD88* L265P somatic mutation in Waldenström's Macroglobulinemia. *N Engl J Med*. 2012;367(9):826-833.
2. Hunter ZR, Xu L, Yang G, et al. The genomic landscape of Waldenström macroglobulinemia is characterized by highly recurring *MYD88* and *WHIM*-like *CXCR4* mutations, and small somatic deletions associated with B-cell lymphomagenesis. *Blood*. 2014;123(11):1637-1646.
3. Yang G, Zhou Y, Liu X, et al. A mutation in *MYD88* (L265P) supports the survival of lymphoplasmacytic cells by activation of Bruton tyrosine kinase in Waldenström macroglobulinemia. *Blood*. 2013;122(7):1222-1232.
4. Jiménez C, Sebastián E, Chillón MC, et al. *MYD88* L265P is a marker highly characteristic of, but not restricted to, Waldenström's macroglobulinemia. *Leukemia*. 2013;27(8):1722-1728.
5. Ngo VN, Young RM, Schmitz R, et al. Oncogenically active *MYD88* mutations in human lymphoma. *Nature*. 2011;470(7332):115-119.

6. Xu L, Hunter ZR, Yang G, et al. Detection of MYD88 L265P in peripheral blood of patients with Waldenström's Macroglobulinemia and IgM monoclonal gammopathy of undetermined significance. *Leukemia*. 2014;28(8):1698-1704.
7. Kaushal A, Nooka AK, Carr AR, et al. Aberrant extrafollicular B cells, immune dysfunction, myeloid inflammation, and MyD88-mutant progenitors precede waldenstrom macroglobulinemia. *Blood Cancer Discov*. 2021;2(6):600-615.
8. Treon SP, Gustine J, Xu L, et al. MYD88 wild-type Waldenstrom Macroglobulinaemia: differential diagnosis, risk of histological transformation, and overall survival. *Br J Haematol*. 2018;180(3):374-380.
9. Paiva B, Corchete LA, Vidriales MB, et al. The cellular origin and malignant transformation of Waldenström macroglobulinemia. *Blood*. 2015;125(15):2370-2380.
10. Treon SP, Tripsas CK, Meid K, et al. Ibrutinib in previously treated waldenström's macroglobulinemia. *N Engl J Med*. 2015;372(15):1430-1440.
11. Tam CS, Opat S, D'Sa S, et al. A randomized phase 3 trial of zanubrutinib vs ibrutinib in symptomatic Waldenström macroglobulinemia: the ASPEN study. *Blood*. 2020;136(18):2038-2050.
12. Guerrero ML, Tsakmaklis N, Xu L, et al. MYD88 mutated and wild-type Waldenström's Macroglobulinemia: characterization of chromosome 6q gene losses and their mutual exclusivity with mutations in CXCR4. *Haematologica*. 2018;103(9):e408-e411.
13. Garcia-Sanz R, Dogliotti I, Zaccaria GM, et al. 6q deletion in Waldenström macroglobulinaemia negatively affects time to transformation and survival. *Br J Haematol*. 2021;192(5):843-852.
14. Campbell PJ, Getz G, Korbel JO, et al. Pan-cancer analysis of whole genomes. *Nature*. 2020;578(7793):82-93.
15. Li Y, Roberts ND, Wala JA, et al. Patterns of somatic structural variation in human cancer genomes. *Nature*. 2020;578(7793):112-121.
16. Bustoros M, Sklaventis-Pistofidis R, Park J, et al. Genomic profiling of smoldering multiple myeloma identifies patients at a high risk of disease progression. *J Clin Oncol*. 2020;38(21):2380-2389, 0(0):JCO.20.00437.
17. Bustoros M, Anand S, Sklaventis-Pistofidis R, et al. Genetic subtypes of smoldering multiple myeloma are associated with distinct pathogenic phenotypes and clinical outcomes. *Nat Commun*. 2022;13(1):3449.
18. Oben B, Froyen G, Maclachlan KH, et al. Whole-genome sequencing reveals progressive versus stable myeloma precursor conditions as two distinct entities. *Nat Commun*. 2021;12(1):1861.
19. Rustad EH, Yellapantula V, Leongamornlert D, et al. Timing the initiation of multiple myeloma. *Nat Commun*. 2020;11(1):1917.
20. Gerstung M, Jolly C, Leshchiner I, et al. The evolutionary history of 2,658 cancers. *Nature*. 2020;578(7793):122-128.
21. Maura F, Bolli N, Angelopoulos N, et al. Genomic landscape and chronological reconstruction of driver events in multiple myeloma. *Nat Commun*. 2019;10(1):3835.
22. Cheng DT, Mitchell TN, Zehir A, et al. Memorial sloan kettering-integrated mutation profiling of actionable cancer targets (MSK-IMPACT): A hybridization capture-based next-generation sequencing clinical assay for solid tumor molecular oncology. *J Mol Diagn*. 2015;17(3):251-264.
23. Zehir A, Benayed R, Shah RH, et al. Mutational landscape of metastatic cancer revealed from prospective clinical sequencing of 10,000 patients. *Nat Med*. 2017;23(6):703-713.
24. Nguyen B, Fong C, Luthra A, et al. Genomic characterization of metastatic patterns from prospective clinical sequencing of 25,000 patients. *Cell*. 2022;185(3):563-575.e511.
25. Cerami E, Gao J, Dogrusoz U, et al. The cBio cancer genomics portal: an open platform for exploring multidimensional cancer genomics data. *Cancer Discov*. 2012;2(5):401-404.
26. Shen R, Seshan VE. FACETS: allele-specific copy number and clonal heterogeneity analysis tool for high-throughput DNA sequencing. *Nucleic Acids Res*. 2016;44(16):e131.
27. Medina-Martinez JS, Arango-Ossa JE, Levine MF, et al. Isabl Platform, a digital biobank for processing multimodal patient data. *BMC Bioinf*. 2020;21(1):549.
28. Jones D, Raine KM, Davies H, et al. cgpCaVEManWrapper: Simple execution of CaVEMan in order to detect somatic single nucleotide variants in NGS data. *Curr Protoc Bioinformatics*. 2016;56:15.10.11-15.10.18.
29. Martincorena I, Raine KM, Gerstung M, et al. Universal patterns of selection in cancer and somatic tissues. *Cell*. 2017;171(5):1029-1041.e1021.
30. Wala JA, Bandopadhyay P, Greenwald NF, et al. SvABA: genome-wide detection of structural variants and indels by local assembly. *Genome Res*. 2018;28(4):581-591.
31. Alexandrov LB, Kim J, Haradhvala NJ, et al. The repertoire of mutational signatures in human cancer. *Nature*. 2020;578(7793):94-101.
32. Maura F, Degasperi A, Nadeu F, et al. A practical guide for mutational signature analysis in hematological malignancies. *Nat Commun*. 2019;10(1):2969.
33. Rustad EH, Nadeu F, Angelopoulos N, et al. mmsig: a fitting approach to accurately identify somatic mutational signatures in hematological malignancies. *Commun Biol*. 2021;4(1):424.
34. Maura F, Petljak M, Lionetti M, et al. Biological and prognostic impact of APOBEC-induced mutations in the spectrum of plasma cell dyscrasias and multiple myeloma cell lines. *Leukemia*. 2018;32(4):1043-1047.
35. Bazarbachi AH, Avet-Loiseau H, Szalat R, et al. IgM-MM is predominantly a pre-germinal center disorder and has a distinct genomic and transcriptomic signature from WM. *Blood*. 2021;138(20):1980-1985.

36. Holmes AB, Corinaldesi C, Shen Q, et al. Single-cell analysis of germinal-center B cells informs on lymphoma cell of origin and outcome. *J Exp Med*. 2020;217(10).
37. Rustad EH, Yellapantula VD, Glodzik D, et al. Revealing the impact of structural variants in multiple myeloma. *Blood Cancer Discovery*. 2020;1(3):258-273. bloodcandisc.0132.2020.
38. Jain MD, Ziccheddu B, Coughlin CA, et al. Whole-genome sequencing reveals complex genomic features underlying anti-CD19 CAR T-cell treatment failures in lymphoma. *Blood*. 2022;140(4):491-503.
39. Maura F, Imielinski M, Xiang JZ, et al. Molecular evolution of classical hodgkin lymphoma revealed through whole genome sequencing of hodgkin and reed-sternberg cells. *Blood*. 2021;138(Supplement 1):805-805.
40. Nadeu F, Mas-de-les-Valls R, Navarro A, et al. IgCaller for reconstructing immunoglobulin gene rearrangements and oncogenic translocations from whole-genome sequencing in lymphoid neoplasms. *Nat Commun*. 2020;11(1):3390.
41. Varettoni M, Zibellini S, Capello D, et al. Clues to pathogenesis of Waldenström macroglobulinemia and immunoglobulin M monoclonal gammopathy of undetermined significance provided by analysis of immunoglobulin heavy chain gene rearrangement and clustering of B-cell receptors. *Leuk Lymphoma*. 2013;54(11):2485-2489.